Gate-dependent spin-torque in a nanoconductor-based spin-valve

Audrey Cottet

Laboratoire Pierre Aigrain, Ecole Normale Supérieure, CNRS (UMR 8551), Université Pierre et Marie Curie, Université D. Diderot, 24 rue Lhomond, F-75231 Paris Cedex 05, France

(Received 5 April 2011; published 1 August 2011)

This paper discusses the spin-torque effect in a spin-valve made out of two ferromagnetic leads connected through a coherent nanoconductor (NC), in the limit where a single channel of the NC lies near the Fermi energy of the leads. Due to quantum interferences inside the NC, the spin-torque presents clear qualitative differences with respect to the case of a multichannel disordered spin-valve. In particular, it can be modulated with the NC gate voltage. In principle, this modulation can be observed experimentally, assuming that the spin-torque affects a ferromagnetic nanodomain in direct contact with the NC.

DOI: 10.1103/PhysRevB.84.054402 PACS number(s): 73.23.−b, 85.75.−d, 72.25.−b

I. INTRODUCTION

The study of spin-dependent transport in ferromagnetic hybrid structures has raised an intense activity in the context of the development of spin electronics, or spintronics.[1] The most simple and illustrative spintronics device is the spin-valve. It consists of two ferromagnetic layers separated by a nonmagnetic spacer, which can be conducting or insulating. The charge current through a spin-valve depends on the relative orientation of the ferromagnets' magnetizations. This so-called magnetoresistance effect has allowed the development of new kinds of field-sensing and magnetic memory devices.[2,3] Conversely, the relative orientation of the ferromagnets' magnetizations can be modified by a spin-torque effect,[4] which corresponds to an absorption of spin currents by the ferromagnets. When the spin-valve spacer is a multichannel disordered metal, the spin-torque appears only at finite bias.[5] In the case of a thin ballistic spacer, a torque due to an indirect exchange coupling between the ferromagnets can also appear in equilibrium conditions, due to a Ruderman-Kittel-Kasuya-Yosida (RKKY) -like interaction.[2,6–9] The theoretical description of transport in spin-valves is now well developed, in both the multichannel ballistic and multichannel diffusive regimes (see, e.g., Refs. 10–12 and 5,13–15).

Recently, a gate-controlled magnetoresistance effect has been observed in spin-valves based on coherent few-channels nanoconductors, such as carbon nanotubes[16–18] or self-assembled InAs quantum dot,[19,20] placed at low temperatures. The portion of nanoconductor between the two contacts is subject to a strong electronic confinement, which leads to the existence of resonant states whose energy can be shifted by using an electrostatic gate. This allows a strong gate modulation of the conductance and magnetoresistance through the device. However, the spin-torque effect in this kind of device has raised little attention so far.[21,22] This paper discusses the spin-torque effect in the case where the spin-valve spacer is a coherent nanoconductor (NC) with a single channel near the Fermi energy of the leads. A noninteracting scattering formalism is used. The torque felt by each ferromagnet varies with the NC gate voltage. The spin activity of the NC/ferromagnet interfaces stems from the spin dependence of interfacial transmission probabilities and from the spin dependence of interfacial scattering phase shifts (SDIPS). I first discuss analytically various limits, in order to emphasize the role of the different parameters and the qualitative differences with the case of multichannel disordered spacers. In the latter case, a finite SDIPS is necessary to obtain an out-of-plane torque component, due to an SDIPS-induced interfacial effective field.[10,14,23–26] However, in the coherent case, this effect can generally not be disentangled from the indirect exchange coupling between the two ferromagnets, which also gives an out-of-plane contribution to the torque. Another striking result is that a Slonczewski in-plane torque can occur even in the limit of spin-independent interfacial transmission probabilities, due to quantum interferences inside the NC, which lead to a SDIPS-induced spin-filtering effect. In the multichannel case, the out-of-plane torque is usually expected to be much smaller than the in-plane torque, because due to fluctuations of the SDIPS from one channel to another, the out-of-plane torque almost averages out.[10,14] In contrast, in a NC-based spin-valve, it is sometimes possible to choose whether the out-of-plane nonequilibrium contribution to the torque is larger or smaller than the in-plane contribution just by changing the NC gate voltage. I finally discuss the measurability of the spin-torque effect in a NC-based spin-valve. It is necessary to assume that the spin-torque affects a nanodomain in direct contact with the NC. This domain can belong to a wider ferromagnetic contact, similar to what is observed for torque experiments realized with quantum point contacts.[27]

Note that the noninteracting scattering model used in this paper can be experimentally relevant in the case where the contacts between the nanoconductor and the ferromagnets have a sufficiently high capacitance. This was clearly the case, for instance, in Ref. 17, which presents magnetoresistance data for a spin-valve made out of a single-wall carbon nanotube with PdNi contacts. The conductance of the device versus bias voltage and gate voltage clearly indicates the absence of interaction effects such as Coulomb blockade. Therefore, the gate variations of the conductance and magnetoresistance through the device could be well interpreted using a noninteracting scattering model similar to the one discussed in the present paper. In the case of contacts with a smaller capacitance, one should use an interacting description, based for instance on an Anderson-like Hamiltonian.

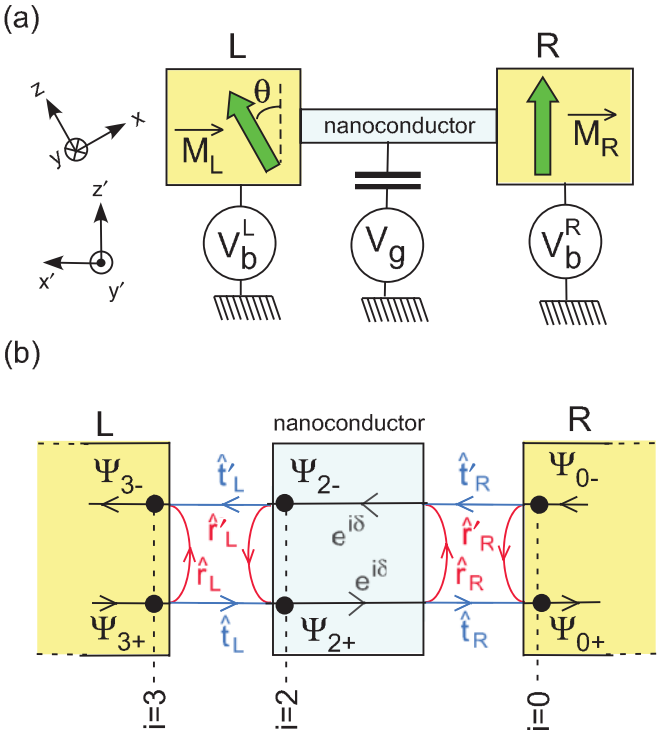

FIG. 1. (Color online) (a) Scheme of the spin-valve device considered in this paper. A ballistic nanoconductor is connected to two ferromagnets L and R with magnetizations $\vec{M}_L$ and $\vec{M}_R$, which form an angle θ. The nanoconductor is capacitively coupled to a gate biased with a voltage V_g. (b) Scattering model of the device for channel m. The interface between the ferromagnet $Q \in \{L,R\}$ and the nanoconductor transmits and reflects electrons with amplitudes $\hat{t}_Q$,$\hat{t}'_Q$ and $\hat{r}_Q$, $\hat{r}'_Q$, which have a 2×2 structure in spin space (see text). The electrons acquire a winding phase δ while they cross the nanoconductors. The right-going/left-going wave function $\Psi_{i\pm}$ at spot $i \in \{0,2,3\}$ is related to the incoming wave functions Ψ_{3+} and Ψ_{0-} by $\Psi_{i\pm} = \Gamma_{i\pm}\Psi_{0-} + \Lambda_{i\pm}\Psi_{3+}$. In the text, we express the spin-torque on L in terms of $\Lambda_{2\pm}$ and $\Gamma_{2\pm}$, and the conductance through the device in terms of Λ_{0+}. In Sec. VI, we assume that $\vec{M}_R$ is fixed, while $\vec{M}_L$ can move. The spin referential $\{x,y,z\}$ is such that $\vec{M}_L = \vec{z}$, while the referential $\{x',y',z'\}$ is fixed with $\vec{M}_R = \vec{z}'$.

II. THEORETICAL MODEL

I consider a spin-valve made out of a NC with length ℓ contacted to two left and right ferromagnetic electrodes L and R [see Fig. 1(a)]. The magnetizations of L and R are noted $\overrightarrow{M_L}$ and $\overrightarrow{M_R}$. The NC chemical potential can be tuned thanks to a capacitive gate biased with a voltage V_g. The dynamics of $\overrightarrow{M_L}$ is affected by a spin-transfer torque $\vec{T}$, which is due to the spin-dependent scattering of electrons by L and R. When $\overrightarrow{M_L}$ and $\overrightarrow{M_R}$ are noncollinear, the spin-current incident on L can have components perpendicular to $\overrightarrow{M_L}$, which are not conserved across L. However, the total momentum of the circuit must be conserved. The torque $\vec{T}$ corresponds to an absorption of the nonconserved spin currents by $\overrightarrow{M_L}$[4]. In real samples, the electronic transport inside L leads to a relaxation of spin collinearly to $\overrightarrow{M_L}$ (transverse spin dephasing) because spin components parallel and antiparallel to $\overrightarrow{M_L}$ quickly lose their coherence with respect to each other when electrons propagate into L.[10,23,24] This occurs on a scale ξ_F called the magnetic-coherence length or transverse spin-dephasing length, which is typically of the order of a nanometer for a ferromagnetic material like Ni.[28–31] Hence, if the length of L exceeds a few nanometers along the transport direction, $\overrightarrow{M_L}$ fully absorbs the perpendicular spin current transmitted into L. In this case, the torque $\vec{T}$ on electrode L corresponds directly to the transverse component of the spin current $\vec{I}_{\text{spin},2}$ just at the right of L, i.e., $\vec{T} = -\vec{I}_{\text{spin},2} + (\vec{I}_{\text{spin},2}\cdot\overrightarrow{M_L})\overrightarrow{M_L}/M_L$.[32] In this picture, it is possible to treat the ferromagnet $Q \in \{L,R\}$ as a fermionic reservoir, i.e., the states with energy E inside Q are populated according to a Fermi distribution $f_Q(E) = 1/\{1+\exp[(E-E_F+eV_b^Q)/k_BT]\}$, with V_b^Q the bias voltage applied to Q and E_F the Fermi energy of the leads.[33]

In this paper, the electronic transport inside the NC is described with the Landauer-Büttiker scattering formalism.[34] The ferromagnetic nature of contact Q is taken into account through the spin dependence of the electronic scattering matrix $\tilde{S}_Q$ between the ferromagnet Q and the NC, and the transverse spin-dephasing hypothesis inside Q. One important specificity of NCs is the strong energy separation between transverse modes. As a result, one can reach a regime where a single mode m of the NC lies near the Fermi energy of the reservoirs (i.e., at a distance smaller than k_BT or the level width). The purpose of this work is to study how the contribution of mode m to the torque $\vec{T}$ evolves with the lead's bias voltages $V_b^{L(R)}$ and the NC gate voltage V_g. From Secs. II to V, the different spin components are given in a referential $\{x,y,z\}$ attached to $\overrightarrow{M_L} = \vec{z}$ [see Fig. 1(a)]. The matrices $\tilde{S}_L$ and $\tilde{S}_R$ can be expressed as $\tilde{S}_L = S_L$ and $\tilde{S}_R = U(\theta)S_RU^{-1}(\theta)$, with, in the scattering space,[34]

$$S_Q = \begin{bmatrix} \hat{r}_Q & \hat{t}'_Q \\ \hat{t}_Q & \hat{r}'_Q \end{bmatrix} \tag{1}$$

for $Q \in \{L,R\}$, and

$$U(\theta) = \begin{bmatrix} \cos\left(\frac{\theta}{2}\right)\hat{\sigma}_0 - i\sin\left(\frac{\theta}{2}\right)\hat{\sigma}_y & 0 \\ 0 & \cos\left(\frac{\theta}{2}\right)\hat{\sigma}_0 - i\sin\left(\frac{\theta}{2}\right)\hat{\sigma}_y \end{bmatrix}. \tag{2}$$

I note $\hat{\sigma}_x$, $\hat{\sigma}_y$, and $\hat{\sigma}_z$ as the Pauli matrices in spin space and $\hat{\sigma}_0$ as the identity matrix in spin space. The reflection and transmission matrices between the ferromagnet Q and the NC, noted $\hat{r}_Q$, $\hat{r}'_Q$, and $\hat{t}_Q$,$\hat{t}'_Q$, respectively, are defined in Fig. 1(b). These matrices have a structure in spin space, i.e.,

$$\hat{r}_Q = \begin{bmatrix} \sqrt{1-T_Q^u}e^{i\varphi_Q^u} & 0 \\ 0 & \sqrt{1-T_Q^d}e^{i\varphi_Q^d} \end{bmatrix}, \tag{3}$$

$$\hat{r}'_Q = \begin{bmatrix} \sqrt{1-T_Q^u}e^{i\bar{\varphi}_Q^u} & 0 \\ 0 & \sqrt{1-T_Q^d}e^{i\bar{\varphi}_Q^u} \end{bmatrix}, \tag{4}$$

and

$$\hat{t}_Q = \hat{t}'_Q = \begin{bmatrix} i\sqrt{T_Q^u}e^{i\frac{\varphi_Q^u+\bar{\varphi}_Q^u}{2}} & 0 \\ 0 & i\sqrt{T_Q^d}e^{i\frac{\varphi_Q^d+\bar{\varphi}_Q^d}{2}} \end{bmatrix}. \quad (5)$$

The number of parameters occurring in S_Q has been minimized by assuming flux conservation and spin conservation along $\overrightarrow{M_Q}$ by the Q/NC interface. The u and d indices refer to majority and minority spin species for each ferromagnet considered. I note $T_Q^{u(d)} = 1 - R_Q^{u(d)}$ as the transmission probability for a majority(minority) spin across contact Q, while $\varphi_Q^{u(d)}$ and $\bar{\varphi}_Q^{u(d)}$ are the reflection phases for majority(minority) spins on the left and right side of the Q/NC interface, respectively. The values of the interfacial transmission phases are imposed by those of the reflection phases, which explains the shape of the phase factors in Eq. (5) (see Ref. 35 for details). Note that the values of the interface parameters $T_Q^{u(d)}$, $\varphi_Q^{u(d)}$, and $\bar{\varphi}_Q^{u(d)}$ are difficult to predict since they can depend on the microscopic details of the ferromagnet/NC contacts. However, they can be considered as fitting parameters that have to be determined for each sample. Such an approach was already used successfully to interpret quantitatively spin-dependent transport experiments in spin-valves and multiterminal circuits based on single-wall carbon nanotubes.[16,17,36] Electrons acquire a winding phase δ while crossing the NC. This phase can be tuned with the NC gate voltage V_g. It also depends on the electronic energy E (see Sec. VI).

The conductance and magnetoresistance corresponding to the above model have already been studied theoretically in Ref. 37. Due to quantum interferences inside the NC, these signals depend on δ and thus on V_g. Reference 21 has discussed the torque in a one-dimensional spin-valve model based on a single channel Blonder-Tinkham-Klapwijk approach.[38] This case is very different from the one discussed in the present paper, since in Ref. 21 the whole ferromagnetic contacts are modeled as delta-function potential barriers that produce no transverse spin dephasing. Reference 22 has used an Anderson-Hamiltonian approach. However, these authors have studied only the in-plane out-of-equilibrium torque and they did not take into account the SDIPS. In the present approach, the ferromagnet/NC interfaces could be alternatively modeled as delta-function potential barriers. However, this would impose a given relation between the interfacial transmissions and scattering phases. Equations (3)–(5) are more general since they can account for any type of interface potential profile. They also allow one to study separately the effects of the spin dependence of the interface transmission probabilities and of the SDIPS. It has been shown that these two properties affect the device conductance G in qualitatively different ways.[37] Qualitative differences are also expected for the spin-torque.

III. GENERAL EXPRESSION OF THE SPIN-TORQUE

For simplicity, one can assume that, at any energy, mode m is not coupled to the other modes of the NC upon scattering by the NC/ferromagnet contacts. In this case, the torque acting on the left magnetization writes $\vec{T} = \vec{T}_m + \vec{C}$, with a separate contribution $\vec{T}_m$ from mode m. The contribution $\vec{C}$ accounts for other modes, which are far from the Fermi energy of the reservoirs. It is convenient to decompose $\vec{T}_m$ as $\vec{T}_m^{\rm eq} + \vec{T}_m^{\rm tr}$, with a finite bias contribution $\vec{T}_m^{\rm tr}$ and an equilibrium term $\vec{T}_m^{\rm eq}$, which exists in the absence of a bias voltage, i.e., when $f_{0(3)}(E) = f_{\rm eq}(E) = 1/\{1 + \exp[(E - E_F)/k_BT]\}$. The parametrization introduced in Sec. II leads to[39]

$$\vec{T}_m^{\rm eq} = \int dE\big[A_{23}^y(E) + A_{20}^y(E)\big] f_{\rm eq}(E)\vec{y} \quad (6)$$

and

$$\vec{T}_m^{\rm tr} = \int dE\, A_{20}^x(E)[f_0(E) - f_3(E)]\vec{x} + \sum_{i\in\{0,3\}} \int dE\, A_{2i}^y(E)[f_i(E) - f_{\rm eq}(E)]\vec{y}, \quad (7)$$

with $A_{20}^{\mu}(E) = {\rm Tr}_\sigma[\sigma_\mu(\Gamma_{2-}\Gamma_{2-}^\dagger - \Gamma_{2+}\Gamma_{2+}^\dagger)]/4\pi$ and $A_{23}^{\mu}(E) = {\rm Tr}_\sigma[\sigma_\mu(\Lambda_{2-}\Lambda_{2-}^\dagger - \Lambda_{2+}\Lambda_{2+}^\dagger)]/4\pi$ for $\mu \in \{x,y\}$. The in-plane and out-of-plane torques correspond to $\vec{x}$ and $\vec{y}$ components, respectively. Here, $\Gamma_{2\mp}$ [$\Lambda_{2\mp}$] are the coefficients obtained when decomposing the left[right]-going wave function associated with m just on the right of L in terms of the modes incoming from L and R [see Fig. 1(b)]. These coefficients can be expressed in terms of the parameters introduced in Sec. II. The trace in the above expressions runs over the spin index σ. We will see in Sec. IV that mode m can contribute to the equilibrium value of the torque ($\vec{T}_m^{\rm eq} \neq 0$) because one has in the general case $A_{23}^y(E) \neq -A_{20}^y(E)$. Since $f_{\rm eq}(E)$ appears in the integrand of Eq. (6), in principle, $\vec{T}_m^{\rm eq}$ depends on the properties of channel m on a wide range of energies for which $T_Q^{u(d)}$, $\varphi_Q^{u(d)}$, and $\bar{\varphi}_Q^{u(d)}$ should be energy dependent. By analogy, $\vec{C}$ can also be finite, although it accounts for the contribution of modes that are far from the Fermi energy of the reservoirs. The full values of $\vec{T}_m^{\rm eq}$ and $\vec{C}$ depend on the whole band structure of the NC and ferromagnets. However, if $V_b^{L(R)}$ and V_g are too small to bring other modes than m close to E_F, $\vec{C}$ can be considered as independent from the gate and bias voltages. The main purpose of this work is to study the gate and bias dependences of the torque, which are contained in $\vec{T}_m = \vec{T}_m^{\rm eq} + \vec{T}_m^{\rm tr}$. Note that when a finite bias voltage V_b is applied to the left reservoir ($V_b^L = V_b$ and $V_b^R = 0$), one obtains, in the low-temperature linear regime $eV_b \ll k_BT \ll T_{L[R]}^{u(d)}\hbar v_F/2\ell$,

$$\vec{T}_m^{\rm tr} = eV_bA_{20}^x\vec{x} - eV_bA_{23}^y\vec{y}\big|_{E=E_F}. \quad (8)$$

This is not equivalent to applying the bias voltage to the right reservoir ($V_b^L = 0$ and $V_b^R = -V_b$), since one finds in this second case

$$\vec{T}_m^{\rm tr} = eV_bA_{20}^x\vec{x} + eV_bA_{20}^y\vec{y}\big|_{E=E_F}. \quad (9)$$

One can check that the expressions of A_{20}^x, A_{20}^y, and A_{23}^y involve a denominator

$$D(\theta) = |\beta_{uu}\beta_{dd}\cos^2(\theta) + \beta_{ud}\beta_{du}\sin^2(\theta)|^2,$$

with $\beta_{ss'} = 1 - e^{i\phi_{s,s'}}\sqrt{R_L^sR_R^{s'}}$, $\phi_{s,s'} = 2\delta + \bar{\varphi}_L^s + \varphi_R^{s'}$, and spin indices $(s,s') \in \{u,d\}^2$ defined in Sec. II. This denominator expresses the fact that electrons are subject to multiple reflections between the two ferromagnets. This leads to resonances that

appear as peaks in the conductance $G = (e^2/\hbar)\mathrm{Tr}_\sigma[\Lambda_{0+}^\dagger \Lambda_{0+}]$ of the spin-valve versus δ (see, for instance, Fig. 3). Similarly, the torque can strongly depend on δ, as shown below.

IV. ANALYTICAL EXPRESSIONS OF THE TORQUE IN VARIOUS LIMITS

This section discusses analytically various limiting cases, which are not necessarily obvious to reach in practice, but allow one to understand the role of the different parameters.

A. Case of a spin-independent *L*/NC contact

I first assume that the scattering matrix $\tilde{S}_L$ describing the contact between the ferromagnet L and the NC is not spin dependent, i.e., $T_L^{u(d)} = T_L = 1 - R_L, \varphi_L^{u(d)} = \varphi_L$, and $\bar{\varphi}_L^{u(d)} = \bar{\varphi}_L$. One finds $A_{20}^y = A_{23}^y = 0$; thus there is no equilibrium torque and no out-of-plane torque in this case. In contrast, one finds a finite out-of-equilibrium in-plane torque ($\vec{T}_m^{\mathrm{tr}} \neq 0$), since

$$A_{20}^x = T_L \frac{\sin(\theta)}{4\pi D(\theta)} \Big[(T_L - 2)\big(T_R^d - T_R^u\big) + 2\sqrt{R_L} \times \Big(\sqrt{R_R^d} T_R^u \cos[\phi_d] - \sqrt{R_R^u} T_R^d \cos[\phi_u] \Big) \Big], \quad (10)$$

with $\phi_{u(d)} = 2\delta + \bar{\varphi}_L + \varphi_R^{u(d)}$. This effect is similar to the spin-filtering torque discussed by Slonczewski.[4] In the present case, the spin filtering is not due to the interface matrix $\tilde{S}_L$, which is spin conserving, but to L itself, since a transverse spin dephasing occurs inside L. Interestingly, the torque can be controlled with the NC gate voltage, since δ occurs in Eq. (10). From the above equation, if $T_R^u = T_R^d = T_R$, the coefficient A_{20}^x remains finite, i.e.,

$$A_{20}^x = \sqrt{R_L R_R} T_L T_R (\cos[\phi_u] - \cos[\phi_d]) \frac{\sin(\theta)}{2\pi D(\theta)}.$$

The existence of a finite torque may seem surprising in this case. Indeed, if the right NC/ferromagnet contact was considered alone (semi-infinite geometry), the current in the NC would not be spin polarized, since $T_R^u = T_R^d$. However, one should keep in mind that quantum interferences occur inside the NC. In the presence of a SDIPS at contact R, the whole F/NC/F device behaves as a spin polarizer along $\overrightarrow{M_R}$, because spins parallel and antiparallel to $\overrightarrow{M_R}$ are resonant inside the NC for different energies.[37] To confirm the crucial role of quantum interferences in this effect, one can check that A_{20}^x vanishes for $T_L = 1$.

B. Case with no SDIPS

I now consider a case where $\tilde{S}_L$ and $\tilde{S}_R$ are both spin dependent, but there is no SDIPS, i.e., $\varphi_{L[R]}^{u(d)} = \varphi_{L[R]}$ and $\bar{\varphi}_{L[R]}^{u(d)} = \bar{\varphi}_{L[R]}$. In this limit, one can check

$$A_{20}^y = \sin[\theta]\sin[2(\delta + \bar{\varphi}_L + \varphi_R)] \times \big[\sqrt{R_L^u}\big(T_L^d - 2\big) - \sqrt{R_L^d}\,\big(T_L^u - 2\big)\big] \times \big(T_R^u \sqrt{R_R^d} - T_R^d \sqrt{R_R^u}\big)/4\pi, \quad (11)$$

$$A_{23}^y = \sin[\theta]\sin[2(\delta + \bar{\varphi}_L + \varphi_R)] \times \big[\sqrt{R_R^u}\big(T_R^d - 2\big) - \sqrt{R_R^d}\big(T_R^u - 2\big)\big] \times \big(T_L^u \sqrt{R_L^d} - T_L^d \sqrt{R_L^u}\big)/4\pi, \quad (12)$$

and, using $T_{L(R)}^{u[d]} = T_{u[d]}$, $\varphi_{L[R]}^{u(d)} = \varphi$, and $\bar{\varphi}_{L[R]}^{u(d)} = \bar{\varphi}$,

$$A_{20}^x = (T_u - T_d)(T_u + T_d - T_u T_d)\sin[\theta]\sin^2[\phi/2]/2\pi, \quad (13)$$

with $\phi = 2\delta + \bar{\varphi} + \varphi$. Interestingly, Eqs. (11) and (12) give $A_{20}^y = A_{23}^y$ for $T_L^{u(d)} = T_R^{u(d)}$. Therefore, one can obtain an out-of-plane contribution to the equilibrium torque without a SDIPS ($\vec{T}_m^{\mathrm{eq}} \neq 0$), even if the NC/ferromagnet contacts are symmetric. This effect is a corollary of the non-local-exchange coupling mediated by itinerant electrons, which has been observed between two ferromagnets connected through a very thin normal metal spacer.[2,6,7] The nonlocal exchange can be explained in terms of a spin-dependent RKKY interaction, which is naturally taken into account by scattering descriptions.[5,9,40] Interestingly, this effect does not occur when the central conductor of the spin-valve is a diffusive metallic electrode,[10] because it vanishes in the limit of a large number of channels in the presence of disorder.[5,14] From Eqs. (11)–(13), the out-of-equilibrium torque has both an in-plane component (Slonczewski-like) and out-of-plane component (related to the interlayer exchange coupling). In contrast, in the case where the conductor placed between the two ferromagnets is a multichannel diffusive conductor, there is no out-of-plane nonequilibrium torque when the SDIPS vanishes.

C. Case of two non-spin-filtering contacts

I now assume that both contacts have spin-independent transmission probabilities, but a finite SDIPS, i.e., $T_{L[R]}^{u(d)} = T_{L[R]} = 1 - R_{L[R]}$. In this case, one finds

$$A_{20}^x = T_L T_R \cos\left[\frac{\bar{\varphi}_L^u - \bar{\varphi}_L^d}{2}\right]\Theta,$$
$$A_{20}^y = (2 - T_L) T_R \sin\left[\frac{\bar{\varphi}_L^u - \bar{\varphi}_L^d}{2}\right]\Theta, \quad (14)$$
$$A_{20}^y - A_{23}^y = 2(T_R - T_L)\sin\left[\frac{\bar{\varphi}_L^u - \bar{\varphi}_L^d}{2}\right]\Theta,$$

and

$$\Theta = \sqrt{R_L R_R}\sin\left[\frac{\varphi_R^d - \varphi_R^u}{2}\right]\sin\left[\frac{\phi_{u,u} + \phi_{d,d}}{2}\right]\frac{\sin(\theta)}{\pi D(\theta)}. \quad (15)$$

Thus there exists out-of-plane contributions to both $\vec{T}_m^{\mathrm{eq}}$ and $\vec{T}_m^{\mathrm{tr}}$. In the multichannel incoherent case, it has already been found that the SDIPS can cause an out-of-plane torque, proportionally to the imaginary part of the so-called "mixing conductance." To understand this effect, one must note that an electron scattered by contact L with a spin noncollinear to $\overrightarrow{M_L}$ precesses around $\overrightarrow{M_L}$ due to $\bar{\varphi}_L^u \neq \bar{\varphi}_L^d$. In other words, the SDIPS causes an effective Zeeman interfacial field along $\overrightarrow{M_L}$. Due to momentum conservation, the electronic precession around this field leads to an out-of-plane torque on L. However, this picture is more delicate to use in the present case

where the existence of an out-of-plane torque $\vec{T}_m^{\rm tr}$ cannot be disentangled from interference effects, because it requires $T_L < 1$. Therefore, the Slonczewski in-plane torque and the out-of-plane indirect exchange effect discussed above also occur.

D. Case of a left perfectly transmitting contact

To suppress quantum interferences inside the NC, one can consider the case $T_L^{u(d)} = 1$. This gives quite generally $A_{20}^y = A_{23}^y = 0$ and

$$A_{20}^x = \left(T_R^u - T_R^d\right)\sin(\theta)/4\pi.$$

Due to the absence of quantum interferences, interfacial reflection phases are not relevant anymore. The contribution of mode m to the torque is purely in-plane. The absence of an out-of-plane torque contribution may seem surprising since the transmission phases from the NC to L can depend on spin [see Eq. (5)]. However, this property has no physical consequence in the present model, because of the transverse spin dephasing occurring in L.

E. Case of a left perfectly reflecting contact

In contrast, the present model gives a purely out-of-plane torque contribution in the limit $T_L^{u(d)} = 0$, which leads quite generally to $A_{20}^x = A_{23}^y = 0$ and

$$A_{20}^y = \frac{\sin(\theta)}{\pi D(\theta)}\left(\left(T_R^u - T_R^d\right)\cos\left[\frac{\bar{\varphi}_L^u - \bar{\varphi}_L^d}{2}\right] - \sqrt{R_R^d}T_R^u\cos\left[\frac{\phi_{u,d}+\phi_{d,d}}{2}\right] + \sqrt{R_R^u}T_R^d\cos\left[\frac{\phi_{u,u}+\phi_{d,u}}{2}\right]\right)\sin\left[\frac{\bar{\varphi}_L^u - \bar{\varphi}_L^d}{2}\right].$$

There is no in-plane torque contribution in this case because electrons cannot cross the L/NC interface, and therefore, the spin-filtering effect considered by Slonczewski is not relevant anymore. One finds $A_{23}^y = 0$ because electrons can enter the device through the right contact only. The torque depends on V_b^R although there is no charge transport. This counterintuitive result can be understood by noting that since $T_L^{u(d)} = 0$, electrons inside the NC remain in equilibrium with the right ferromagnet. In this case, changing V_b^R instead of V_g just gives another way to observe the variations of an equilibrium torque. The SDIPS-induced interface exchange field at the left contact plays a crucial role in the establishment of this torque since $A_{20}^y = 0$ for $\bar{\varphi}_L^u = \bar{\varphi}_L^d$.

V. ANGULAR AND GATE DEPENDENCE OF THE OUT-OF-EQUILIBRIUM PART OF THE TORQUE

As already explained in Sec. III, the absolute value of the torque felt by L depends on the whole band structure of the NC and ferromagnets. The purpose of this article is not to calculate this value, but the gate and bias dependences of the torque, for small applied voltages. If $V_b^{L(R)}$ and V_g are too small to bring other modes than m close to E_F, they can modify significantly the torque contribution $\vec{T}_m$ from mode m only.

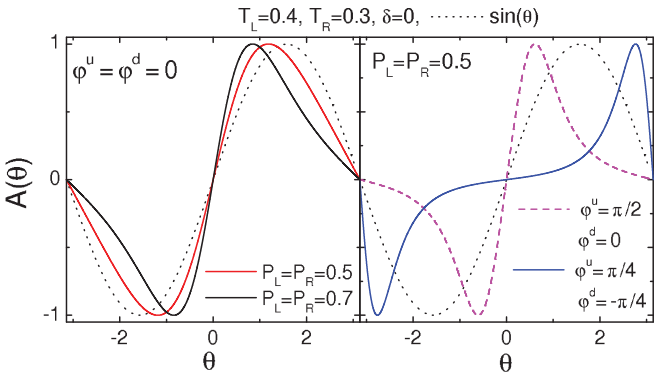

FIG. 2. (Color online) Function $A(\theta)$ giving the angular dependence of $\vec{T}_m^{\rm tr}$ in the low-temperature and linear-bias limit. The left panel shows the effect of a variation in the spin-polarization $P_{L[R]}$ of the interface tunnel probabilities, in the absence of a SDIPS ($\varphi^u = \varphi^d$). The right panel shows the effect of a variation in the spin-averaged reflection phase $(\varphi^u + \varphi^d)/2$, for a finite and constant SDIPS $\varphi^u - \varphi^d = \pi/2$. For comparison, the function $\sin[\theta]$ is shown with dotted lines in both panels.

Using constant values for $T_Q^{u(d)}$, $\varphi_Q^{u(d)}$, and $\bar{\varphi}_Q^{u(d)}$ is a reasonable assumption in this context. In practice, one can check, using realistic parameters, that the variations of $\vec{T}_m^{\rm eq}$ with V_g are likely to be small (see Sec. VI). Therefore, I have chosen to focus on the angular and gate dependence of $\vec{T}_m^{\rm tr}$. In this section and the following, I use $T_{L[R]}^{u(d)} = T_{L[R]}(1 \pm P_{L[R]})$. From the previous section, one can check that the only physically relevant phases are the reflection phases inside the NC, i.e., $\bar{\varphi}_L^{u(d)}$ and $\varphi_R^{u(d)}$. I use below $\varphi_{L(R)}^{u(d)} = \bar{\varphi}_{L(R)}^{u(d)} = \varphi^{u(d)}$.

For simplicity, I discuss the angular dependence of $\vec{T}_m^{\rm tr}$ in the low-temperature linear regime [see Eqs. (8) and (9)]. This dependence can be characterized with the function $A(\theta) = [\sin(\theta)/D(\theta)]/\max_\theta[\sin(\theta)/D(\theta)]$. Indeed, in the different cases considered analytically in Sec. IV, the coefficients A_{20}^x, A_{20}^y, and A_{23}^y are proportional to $\sin(\theta)/D(\theta)$. I have checked analytically that this property remains true even if no particular hypotheses are made on $\tilde{S}_L$ and $\tilde{S}_R$. The spin-torque is often nonsinusoidal in the multichannel disordered case (see, e.g., Ref. 5). In the present case, when $T_L^{u(d)}$ and $T_R^{u(d)}$ are close to 1, one finds $D(\theta) \to 1$, so that $A(\theta) = \sin(\theta)$ to a good approximation. In the absence of a SDIPS and for $T_L^{u(d)}$ and $T_R^{u(d)}$ close to zero, one finds $D(\theta) \to (1 - e^{i\phi})^2$ with $\phi_{s,s'} = \phi$, so that $A(\theta) = \sin(\theta)$ again. In order to have a nonsinusoidal $A(\theta)$ for small values of $T_{L[R]}^{u(d)}$, a finite SDIPS must be used. However, it is also possible to have a nonsinusoidal $A(\theta)$ for a vanishing SDIPS by using intermediate values for $T_{L[R]}^{u(d)}$. The left panel of Fig. 2 shows $A(\theta)$ in the absence of a SDIPS. An increase in $P_{L[R]}$ can help to increase the anharmonicity of $A(\theta)$. From the right panel of Fig. 2, it nevertheless seems that a strong SDIPS more easily leads to a strongly nonsinusoidal $A(\theta)$. The anharmonicity of $A(\theta)$ can also be changed with δ (not shown) and with the value of the spin-averaged reflection phases $(\varphi_{L(R)}^u + \varphi_{L(R)}^d)/2$ (see right panel of Fig. 2).

I now discuss the δ dependence of $\vec{T}_m^{\rm tr}$ in the low-temperature linear regime. This dependence is given by the coefficients A_{20}^x, A_{20}^y, and A_{23}^y, which are shown in Fig. 3, for

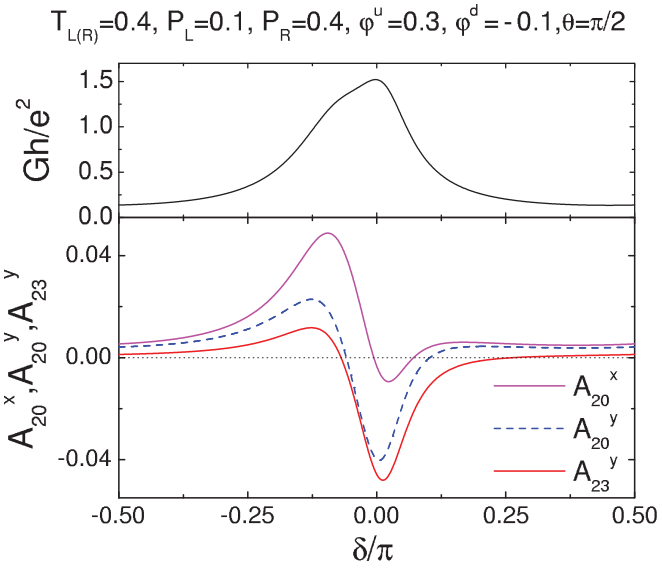

FIG. 3. (Color online) Conductance G (top panel) and coefficients A^x_{20}, A^y_{20}, and A^y_{23} determining the low-temperature linear-bias limit of $T^{\rm tr}_m$ (bottom panel), as a function of the winding phase δ through the NC.

a particular set of interface parameters. These coefficients are π periodic with δ. Remarkably, they can change sign with δ. In the multichannel case, the out-of-plane torque is usually expected to be much smaller than the in-plane torque, because due to fluctuations of the SDIPS from one channel to another, the out-of-plane torque almost averages out.[10,14,26] However, in the present case, $|A^y_{20}|$ and $|A^y_{23}|$ can be smaller or larger than $|A^x_{20}|$ depending on the value of δ considered (see bottom panel of Fig. 3). To illustrate the effects of the SDIPS and of the polarization $P_{L(R)}$ of the interfacial tunnel probabilities, Fig. 4 shows the coefficients A^x_{20}, A^y_{20}, and A^y_{23} for the same parameters as in Fig. 3, but with $\varphi^u = \varphi^d$ (no SDIPS) in the left panel and $P_{L(R)} = 0$ in the right panel. In the right panel, one has exactly $A^y_{20} = A^y_{23}$ due to $T_L = T_R$ (see Sec. IV C). In the left panel, A^y_{20} and A^y_{23} are not exactly equal, but the difference is too small to be visible on the scale of the figure, because the spin-dependent transmission probabilities $T_L(1 \pm P_L)$ are relatively close to $T_R(1 \pm P_R)$ (see Sec. IV B). In general, using a finite SDIPS allows one to increase strongly the amplitude of the torque variations, because the SDIPS tends to induce a spin splitting of electronics resonances inside the NC, which strongly spin polarizes the current through the NC [compare Fig. 4 (left) with Fig. 3]. Of course, increasing $P_{L(R)}$ also allows one to increase the magnitude of the torque [compare Fig. 4 (right) with Fig. 3]. However, a comparison between the left and right panels of Fig. 4 illustrates that the effects of a finite $P_{L(R)}$ and a finite SDIPS on the torque are qualitatively different, since the variations of A^x_{20}, A^y_{20}, and A^y_{23} with δ are different in these two panels. Remarkably, in the left panel, A^x_{20} remains positive for any value of δ, whereas it changes sign with δ in the right panel.

VI. MEASURABILITY OF THE TORQUE IN A COLLINEAR GEOMETRY

This section discusses the measurability of the spin-torque felt by L in a simple collinear configuration. I assume that $\overrightarrow{M_R} = M_R \vec{z}'$ is fixed along a direction $\vec{z}'$, which corresponds to the anisotropy axis of contact L. When one starts from an initial state $\overrightarrow{M_L} = \pm M_L \overrightarrow{z}'$, i.e., $\theta = 0/\pi$ or $\overrightarrow{z} = \pm\vec{z}'$, the spin-torque vanishes. However, Slonczewski has shown that it is possible to observe the spin-torque effect by studying the hysteretic switching of $\overrightarrow{M_L}$ between $\theta = 0$ and $\theta = \pi$, when a ramping magnetic field $\overrightarrow{H}$ is applied collinearly to $\overrightarrow{z}'$. Indeed, since θ must pass continuously between 0 and π during the switching process, the torques can modify the critical switching fields. For simplicity, I consider a range of parameters where the torque is approximately sinusoidal, i.e., $T^{x(y)}_m \propto \sin[\theta]$. In the framework of a Landau-Gilbert equation (see the Appendix), the torque produces an asymmetry $\Delta H_{\rm sw} = (H_{\rm sw+} + H_{\rm sw-})/2$ of the switching fields $H_{\rm sw+}$ and $H_{\rm sw-}$ obtained for increasing and decreasing fields, which can be expressed as

$$\Delta H_{\rm sw} = \left(\alpha^{-1}\, T^x_m\big|_{\theta=\pi/2} - T^y_m\big|_{\theta=\pi/2}\right)/\mu_0 M_L. \qquad (16)$$

Equation (16) involves a Gilbert damping dimensionless constant α, which characterizes the damping of the left magnetization. I will use below the value $\alpha = 0.045$, which has been measured for nickel.[41] The constant α increases the effect of the in-plane torque T^x_m with respect to that of the out-of-plane torque T^y_m.

To motivate experiments, it is interesting to discuss whether the variations of $T^{x(y)}_m$ with the bias or gate voltages are observable through $\Delta H_{\rm sw}$. Since $\Delta H_{\rm sw}$ scales with the inverse of the magnetization M_L, the magnitude of M_L must not be too large. I will assume that the ferromagnet L corresponds to a small magnetic domain in direct contact with the NC. This domain itself can belong to a larger ferromagnetic contact, as observed, for instance, in spin-torque experiments

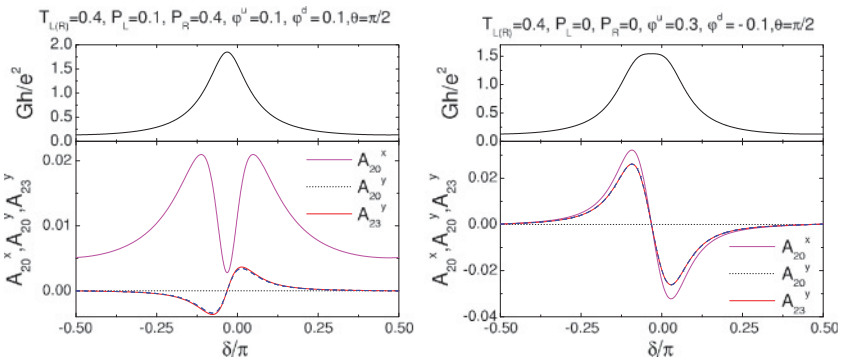

FIG. 4. (Color online) Conductance G and coefficients A^x_{20}, A^y_{20}, and A^y_{23}, as a function of δ. The parameters used here are the same as in Fig. 3, except $\varphi^u = \varphi^d$ (no SDIPS) in the left panels, and $P_{L(R)} = 0$ in the right panels.

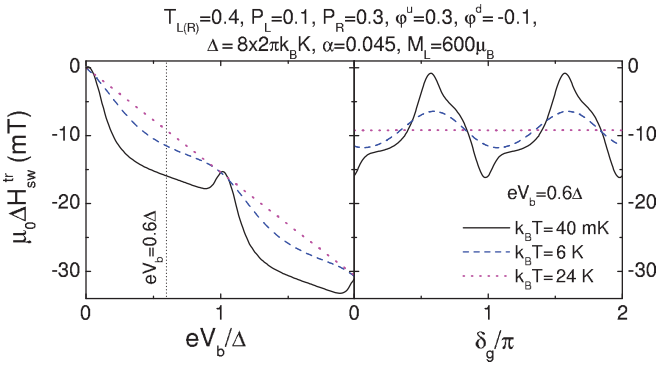

FIG. 5. (Color online) Spin-torque-induced asymmetry $\Delta H_{\rm sw}^{\rm tr}$ of the switching fields, in the case where a finite bias voltage V_b is applied to the left reservoir of the spin-valve. The left and right panel show the variations of $\Delta H_{\rm sw}^{\rm tr}$ with V_b and the gate-controlled phase δ_g, respectively. The curves are shown for various temperatures. It is assumed that the role of L is played by a nickel cubic domain with a side of 2.2 nm, which corresponds to $M_L \simeq 600\mu_B$.

realized with quantum point contacts.[27] Here, I consider a nickel cubic domain with a side of 2.2 nm. In spite of this small size, I disregard Coulomb blockade effects or size-quantization effects inside the domain,[42] since it is assumed to belong to a larger ferromagnetic contact. The Ni domain encloses about 1000 atoms[43] and has thus a magnetization $M_L = 600\mu_B$, with μ_B the Bohr magneton. The transverse spin-dephasing length in Ni is of the order of a nanometer, as revealed by the superconducting proximity effect observed in this material.[28–31] Therefore, the transverse spin-dephasing hypothesis used in this paper seems relevant. Besides, since the NC is in the few-channels transport regime, I assume that conduction through the device is limited by the NC/nanodomain contact. In these conditions, it is reasonable to treat the nanodomain as an electronic reservoir in equilibrium with V_b^L.

I use a quadratic band model for the NC, which yields, after a linearization around the Fermi energy, $\delta = \delta_g + (E - E_F)\pi/\Delta$ with $\delta_g = k_F\ell + (e\eta V_g\pi/\Delta)$ the phase acquired by an electron with energy E_F along the NC. The phase δ_g can be tuned with V_g, through a transduction coefficient η. The parameter $\Delta = h v_F/2\ell$ corresponds to the orbital level spacing inside the NC. Both thermal regimes $\Delta > k_BT$ and $\Delta < k_BT$ can be reached in practice. I assume that the finite bias voltage V_b is applied to the left reservoir ($V_b^L = V_b$ and $V_b^R = 0$). I first discuss the contribution $\Delta H_{\rm sw}^{\rm tr}$ of $\vec{T}_m^{\rm tr}$ to $\Delta H_{\rm sw}$. In practice, this quantity can be determined by measuring the difference between the switching fields for $V_b = 0$ and V_b finite. Figure 5 shows $\Delta H_{\rm sw}^{\rm tr}$ for a given set of interface parameters and a realistic value for Δ.[44] Due to the value of α used, $\Delta H_{\rm sw}^{\rm tr}$ is dominated by the T_m^x term (T_m^x and T_m^y have comparable amplitudes for the parameters of Fig. 5). The left panel of Fig. 5 shows the dependence of $\Delta H_{\rm sw}^{\rm tr}$ on V_b. At low temperatures (i.e., temperatures smaller than the scales of variation of A_{20}^x, A_{20}^y, and A_{23}^y with energy), this dependence is nonlinear, due to resonances occurring inside the NC. Besides, the right panel of Fig. 5 shows that $\Delta H_{\rm sw}^{\rm tr}$ oscillates with δ_g. The amplitude of these oscillations is about 15 mT for the parameters used. In practice, this effect should be measurable if the switchings of the left magnetic domain are sufficiently sharp, like observed with single-wall carbon nanotubes contacted with ferromagnets.[36,45,46] Note that, being conservative, I have used a relatively small SDIPS and small polarizations $P_{L(R)}$ for estimating $\Delta H_{\rm sw}^{\rm tr}$. In principle, $\Delta H_{\rm sw}^{\rm tr}$ can be increased significantly by breaking these restrictions. At larger temperatures, $\Delta H_{\rm sw}^{\rm tr}$ increases linearly with V_b and $\Delta H_{\rm sw}^{\rm tr}$ does not oscillate anymore with δ_g.

I now discuss briefly the contribution $\Delta H_{\rm sw}^{\rm eq}$ of $\vec{T}_m^{\rm eq}$ to $\Delta H_{\rm sw}$. With the parameters of Fig. 5 (right) at low temperatures, the oscillations of $\Delta H_{\rm sw}^{\rm eq}$ with δ_g have an amplitude of about 0.2 mT (not shown); thus $\Delta H_{\rm sw} \simeq \Delta H_{\rm sw}^{\rm tr}$. Therefore, the gate-induced variations of the equilibrium torque component in a NC-based spin-valve are probably difficult to measure in practice.

Note that in Fig. 5 (right) one has $V_b \simeq 2.6$ mV. In these conditions, the coherent scattering approach of this paper is relevant. In order to obtain a current-induced reversal of $\overrightarrow{M_L}$ with no external magnetic field, stronger bias voltages are necessary. In the latter case, one may have to take into account heating and decoherence effects inside the NC.

VII. CONCLUSION

In this paper, I have discussed the spin-torque effect in a spin-valve made out of two ferromagnetic leads connected through a coherent NC. I have assumed that the NC has a single channel near the Fermi energy of the leads. In this case, the spin-torque effect presents many qualitative differences with respect to the case of a multichannel disordered spin-valve. I have discussed the SDIPS-induced interface exchange field, the RKKY-like interlayer exchange coupling, and the Slonczewski spin filtering that occur in this device. The contributions of these three effects to the spin-torque can generally not be disentangled, due to interference effects occurring inside the NC. One interesting specificity of a NC-based spin-valve is that the spin-torque can be modulated with the NC gate voltage. In principle, this modulation can be observed experimentally by studying the hysteretic behavior of the spin-valve with a magnetic field, for instance. This requires one to assume that the torque affects a ferromagnetic nanodomain in direct contact with the NC and belonging, for instance, to a wider lithographically defined ferromagnetic contact.

In relation to this work, it is interesting to point out that there also exists great qualitative differences between the few-channels coherent case and the multichannel disordered case in the context of nonlocal spin transport in a conductor connected to four contacts with colinear magnetizations.[36,47]

ACKNOWLEDGMENTS

I acknowledge discussions with A.-D. Crisan, T. Kontos, André Thiaville, and X. Waintal. This work was financially supported by the ANR under Contract HYFONT No. 09-NANO-002.

APPENDIX

This appendix discusses the dynamics of $\overrightarrow{M_L}$ in the collinear configuration defined in Sec. VI. The modulus M_L of the magnetization $\overrightarrow{M_L} = M_L\overrightarrow{m_L}$ is assumed to be constant ($|\overrightarrow{m_L}| = 1$). To model the dynamics of $\overrightarrow{m_L}$, one can use a Landau-Lifshitz-Gilbert equation,[4]

$$\frac{d\overrightarrow{m_L}}{dt} = -\gamma_0\overrightarrow{m_L}\wedge H\overrightarrow{z}' - \gamma_0 H_u(\overrightarrow{z}\cdot\overrightarrow{m_L})\overrightarrow{m_L}\wedge\overrightarrow{z}' + \tau_\parallel\overrightarrow{m_L}\wedge(\overrightarrow{m_R}\wedge\overrightarrow{m_L}) + \tau_\perp\overrightarrow{m_R}\wedge\overrightarrow{m_L} + \alpha\overrightarrow{m_L}\wedge\frac{d\overrightarrow{m_L}}{dt}, \tag{A1}$$

with $\gamma_0 = -\mu_0\gamma > 0$, $\gamma \simeq -e/m_e$ the gyromagnetic ratio of electrons, and μ_0 the vacuum permeability. The uniaxial anisotropy field of the left ferromagnet is noted $H_u\overrightarrow{z}'$. The torque components T_m^x and T_m^y occur through $\tau_\parallel = T_m^x\gamma/M_L\sin(\theta)$ and $\tau_\perp = -T_m^y\gamma/M_L\sin(\theta)$. The Gilbert damping term is proportional to the dimensionless constant α, and usually fulfills $\alpha \ll 1$. One can look for solutions of Eq. (A1) with the form $\overrightarrow{m_L} = [\sin(\theta)\cos(\omega t), \sin(\theta)\sin(\omega t), \cos(\theta)]$ in the fixed referential $\{x', y', z'\}$. Following Ref. 4, one can assume $\omega \gg d\theta/dt$, i.e., the precession of $\overrightarrow{M_L}$ around the $\overrightarrow{z}'$ axis is much faster than its relaxation toward $\pm\overrightarrow{z}$. This gives $\omega = H\gamma_0 + \tau_\perp + H_u\gamma_0\cos(\theta)$ and

$$\frac{d\theta}{dt} = -\left[\tau_\parallel + \alpha\tau_\perp + \alpha\gamma_0 H + H_u\alpha\gamma_0\cos(\theta)\right]\sin(\theta) = F(\theta). \tag{A2}$$

Equation (A2) corresponds to the dynamics of a fictitious massless damped particle in an effective potential $U(\theta)$, such that $F(\theta) = -\partial U(\theta)/\partial\theta$. From Eq. (A2), the shape of the barrier separating the positions $\theta = 0$ and $\theta = \pi$ depends on the torques. Here, I assume that T_m^x and T_m^y are approximately sinusoidal, so that $\tau_\perp$ and $\tau_\parallel$ can be treated as constants. In this case, $\overrightarrow{m_L}$ can switch from $\pm\overrightarrow{z}$ to $\mp\overrightarrow{z}$ if H decreases/increases until it reaches the value $H_{sw\pm} = \mp H_u - [(\tau_\parallel/\alpha) + \tau_\perp]/\gamma_0$.

[1] G. A. Prinz, Science **282**, 1660 (1998).
[2] M. N. Baibich, J. M. Broto, A. Fert, F. NguyenVan Dau, F. Petroff, P. Etienne, G. Creuzet, A. Friederich, J. Chazelas, Phys. Rev. Lett. **61**, 2472 (1988).
[3] G. Binasch, P. Grünberg, F. Saurenbach, and W. Zinn, Phys. Rev. B **39**, 4828 (1989).
[4] J. C. Slonczewski, J. Magn. Magn. Mater. **159**, L1 (1996).
[5] X. Waintal, E. B. Myers, P. W. Brouwer, and D. C. Ralph, Phys. Rev. B **62**, 12317 (2000).
[6] P. Grünberg, R. Schreiber, Y. Pang, M. B. Brodsky, and H. Sowers, Phys. Rev. Lett. **57**, 2442 (1986).
[7] S. S. P. Parkin, N. More, and K. P. Roche, Phys. Rev. Lett. **64**, 2304 (1990).
[8] D. M. Edwards, J. Mathon, R. B. Muniz, and M. S. Phan, Phys. Rev. Lett. **67**, 493 (1991); K. B. Hathaway and J. R. Cullen, J. Magn. Magn. Mater. **104**, 1840 (1992); P. Bruno and C. Chappert, Phys. Rev. Lett. **67**, 1602 (1991); D. M. Edwards, A. M. Robinson, and J. Mathon, J. Magn. Magn. Mater. **140**, 517 (1995).
[9] X. Bai and L. Zeng, Phys. Rev. B **39**, 10 (1989); J. C. Slonczewski, J. Magn. Magn. Mater. **126**, 374 (1993); P. Bruno, Phys. Rev. B **52**, 411 (1995).
[10] M. D. Stiles and A. Zangwill, Phys. Rev. B **66**, 014407 (2002).
[11] K. M. Schep, P. J. Kelly, and G. E. W. Bauer, Phys. Rev. Lett. **74**, 586 (1995).
[12] P. M. Haney, D. Waldron, R. A. Duine, A. S. Núñez, H. Guo, and A. H. MacDonald, Phys. Rev. B **75**, 174428 (2007).
[13] T. Valet and A. Fert, Phys. Rev. B **48**, 7099 (1993).
[14] A. Brataas, G. E. W. Bauer, and P. J. Kelly, Phys. Rep. **427**, 157 (2006).
[15] V. S. Rychkov, S. Borlenghi, H. Jaffres, A. Fert, and X. Waintal, Phys. Rev. Lett. **103**, 066602 (2009).
[16] S. Sahoo, T. Kontos, J. Furer, C. Hoffmann, M. Gräber, A. Cottet, and C. Schönenberger, Nature Phys. **1**, 99 (2005).
[17] H. T. Man, I. J. W. Wever, and A. F. Morpurgo, Phys. Rev. B **73**, 241401 (2006).
[18] A. Cottet, T. Kontos, S. Sahoo, H. T. Man, M.-S. Choi, W. Belzig, C. Bruder, A. F. Morpurgo, and C. Schönenberger, Semicond. Sci. Technol. **21**, S78 (2006).
[19] K. Hamaya, M. Kitabatake, K. Shibata, M. Jung, M. Kawamura, K. Hirakawa, T. Machida, S. Ishida, and Y. Arakawa, Appl. Phys. Lett. **91**, 022107 (2007).
[20] K. Hamaya, S. Masubuchi, M. Kawamura, T. Machida, M. Jung, K. Shibata, K. Hirakawa, T. Taniyama, S. Ishida, and Y. Arakawa, Appl. Phys. Lett. **90**, 053108 (2007).
[21] F. Romeo and R. Citro, Phys. Rev. B **81**, 045307 (2010).
[22] H.-F. Mu, G. Su, and Q.-R. Zheng, Phys. Rev. B **73**, 054414 (2006).
[23] A. Brataas, Yu. V. Nazarov, and G. E. W. Bauer, Phys. Rev. Lett. **84**, 2481 (2000).
[24] A. Brataas, Yu. V. Nazarov, J. Inoue, and G. E. W. Bauer, Eur. Phys. J. B **9**, 421 (1999).
[25] D. H. Hernando, Yu. V. Nazarov, A. Brataas, and G. E. W. Bauer, Phys. Rev. B **62**, 5700 (2000).
[26] K. Xia, P. J. Kelly, G. E. W. Bauer, A. Brataas, and I. Turek, Phys. Rev. B **65**, 220401(R) (2002).
[27] T. Y. Chen, Y. Ji, C. L. Chien, and M. D. Stiles, Phys. Rev. Lett. **93**, 026601 (2004).
[28] V. T. Petrashov, I. A. Sosnin, I. Cox, A. Parsons, and C. Troadec, Phys. Rev. Lett. **83**, 3281 (1999).
[29] J. W. A. Robinson, S. Piano, G. Burnell, C. Bell, and M. G. Blamire, Phys. Rev. Lett. **97**, 177003 (2006).
[30] Y. Blum, A. Tsukernik, M. Karpovski, and A. Palevski, Phys. Rev. Lett. **89**, 187004 (2002).
[31] V. Shelukhin, A. Tsukernik, M. Karpovski, Y. Blum, K. B. Efetov, A. F. Volkov, T. Champel, M. Eschrig, T. Löfwander, G. Schön, and A. Palevski, Phys. Rev. B **73**, 174506 (2006).

[32]This approach differs from the scattering approach of Refs. 4 and 5, where the ferromagnet L is not treated as a reservoir and the torque is calculated as the difference of the spin currents at the left and right sides of L. However, in the limit of a strong transverse spin dephasing, such complications are not necessary.[10,23,24]

[33]I note e the absolute value of the electron charge ($e > 0$).

[34]Ya. M. Blanter and M. Büttiker, Phys. Rep. **336**, 1 (2000).

[35]A. Cottet, D. Huertas-Hernando, W. Belzig, and Y. V. Nazarov, Phys. Rev. B **80**, 184511 (2009).

[36]C. Feuillet-Palma, T. Delattre, P. Morfin, J.-M. Berroir, G. Fève, D. C. Glattli, B. Plaçais, A. Cottet, and T. Kontos, Phys. Rev. B **81**, 115414 (2010).

[37]A. Cottet, T. Kontos, W. Belzig, C. Schönenberger, and C. Bruder, Europhys. Lett. **74**, 320 (2006).

[38]G. E. Blonder, M. Tinkham, and T. M. Klapwijk, Phys. Rev. B **25**, 4515 (1982).

[39]Using the definitions below Eq. (7), the parametrization introduced in Sec. II leads to $A^x_{23} = -A^x_{20}$.

[40]J. Xiao, G. E. W. Bauer, and A. Brataas, Phys. Rev. B **77**, 224419 (2008).

[41]J. Walowski, M. Djordjevic Kaufmann, B. Lenk, C. Hamann, J. McCord, and M. Münzenberg, J. Phys. D: Appl. Phys. **41**, 164016 (2008).

[42]X. Waintal and O. Parcollet, Phys. Rev. Lett. **94**, 247206 (2005); O. Parcollet and X. Waintal, Phys. Rev. B **73**, 144420 (2006).

[43]Nickel has a face-centered-cubic structure with a lattice parameter of about 0.35 nm.

[44]In a quantum dot made out of a single-wall carbon nanotube section confined between two contacts, $v_F = 8 \times 10^5\ \mathrm{m\,s^{-1}}$ and $\ell = 400$ nm lead to $\Delta = 7.6 \times 2\pi\ k_B$ K.

[45]H. Aurich *et al.*, Appl. Phys. Lett. **97**, 153116 (2010).

[46]It has been checked from magnetic force microscope (MFM) characterizations that the contacts used in Ref. 36 presented many small magnetic domains. This did not prevent the appearance of sharp switchings.

[47]A. Cottet, C. Feuillet-Palma, and T. Kontos, Phys. Rev. B **79**, 125422 (2009).